Elevated Temperature Strength and Room-Temperature Toughness of Directionally Solidified Ni-33Al-33Cr-1Mo

J. DANIEL WHITTENBERGER, S.V. RAJ, IVAN E. LOCCI, and JONATHAN A. SALEM

The eutectic composition Ni-33Al-33Cr-1Mo has been directionally solidified (DS) *via* a modified Bridgman technique at rates ranging from 7.6 to 508 mm/h to determine if the growth rate affects the mechanical properties. Microstructural examination revealed that all DS rods had grain/cellular microstructures containing alternating plates of NiAl and Cr alloyed with Mo. At slower growth rates ($\leq$12.7 mm/h), the grains had sharp boundaries, while faster growth rates ($\geq$25.4 mm/h) led to cells bounded by intercellular regions. None of the growth conditions resulted in either dendrites or third phases. Compressive testing between 1200 and 1400 K indicated that alloys DS at rates between 25.4 and 254 mm/h possessed the best strengths, while room-temperature toughness exhibited a plateau of about 16 MPa$\sqrt{m}$ for growth rates between 12.7 and 127 mm/h. Thus, a growth rate of 127 mm/h represents the best combination of fast processing and mechanical properties for this system.

I. INTRODUCTION

NEW materials are required for the hot sections of the next generation of gas turbine engines. These materials must be able to withstand severe oxidizing conditions and relatively high stresses at temperatures at or exceeding 1300 K. Additionally, the materials must exhibit a tolerance for being handled and subjected to foreign object damage at low temperatures. Any new material, also, should have a lower density than current Ni-base superalloys to reduce the forces developed through rotation and to lower the overall weight of the engine. Based on these requirements, the B2 structure intermetallic NiAl is an attractive candidate for the development of new gas turbine engine material. Its density is about 75 pct of the value for superalloys, its congruent melting point is ~250 K higher than that of superalloys, and NiAl readily forms a protective, slow growing alumina oxide scale. Unfortunately, along with these positive characteristics, NiAl is weak at high temperatures and exhibits low fracture toughness at room temperature.

The simultaneous improvement of elevated temperature strength and room-temperature toughness in NiAl is possible through directional solidification of NiAl-base eutectic alloys.[1–4] However, attainment of these benefits might require a perfectly aligned and fault free directionally solidified (DS) microstructure. In general, such ideal microstructures necessitate slow growth rates that lessen the commercial opportunities for gas turbine engine applications. As part of an effort at the Glenn Research Center to develop NiAl materials with acceptable toughness and strength values, several systems centered on the base NiAl-34Cr (at. pct) eutectic composition are being studied in detail. This base alloy was selected because (1) Cr possesses some inherent oxidation resistance and a reasonably low density, (2) the eutectic melting point of the NiAl-34Cr eutectic is only about 150 K less than the ~1900 K congruent melting point for NiAl,[5] and (3) preliminary work[2] has shown that this eutectic possessed significantly improved 1300 K strength and room-temperature fracture toughness when compared to NiAl.

The present article describes the results from room-temperature fracture toughness and 1200 to 1400 K compressive testing of a Ni-33Al-33Cr-1Mo eutectic, which had been DS at rates ranging from 7.6 to 508 mm/h. This particular system was chosen because replacement of 0.7 at. pct or more Cr by Mo changes the morphology of the second phase from Cr fibers to Cr(Mo) plates,[6] which could improve both the fracture toughness and elevated temperature creep strength.[7,8] Additionally, compression testing was used to determine elevated temperature strength because (1) of the ease of machining and testing specimens and (2) the fact that identical compressive and tensile flow stress-strain rate-temperature properties have been measured in several other DS NiAl-X systems.[9,10] This work extends the preliminary results from the 1300 K compressive testing of as-cast and DS forms of Ni-33Al-33Cr-1Mo reported in Reference 11.

II. EXPERIMENTAL PROCEDURES

Prior to directional solidification, bars of 33Ni-33Al-33Cr-1Mo were prepared by induction melting appropriate amounts of Al, Cr, Ni, and Ni-50Mo in high-purity alumina crucibles under an Ar atmosphere and casting into a split copper chill mold containing two cylindrical cavities 19 mm in diameter by 178 mm in length. Once cooled, the bars were removed, cropped, and placed in a 19.1-mm i.d., high-purity alumina, open ended tube for directional solidification in a modified Bridgman apparatus. Directional solidification was undertaken in flowing high-purity argon, where each as-cast 33Ni-33Al-33Cr-1Mo bar was superheated to 1855 ± 15 K through induction heating of a susceptor. During DS, the molten metal temperature was continuously monitored by a type C W/Re thermocouple in a protective ceramic tube inserted at the midpoint of the melt. Once the metal was melted and the temperature stabilized, the Al_2O_3 tube containing the molten alloy was

J. DANIEL WHITTENBERGER, Materials Engineer, and S.V. RAJ, Materials Engineer, Materials Division, IVAN E. LOCCI, Principal Investigator, Materials Division, Case Western University Reserve University, and JONATHAN A. SALEM, Structural Engineer, Structures and Acoustics Division, are with the NASA-Glenn Research Center, Cleveland, OH 44135. Contact e-mail: John.D.Whittenberger@grc.nasa.gov

Manuscript submitted September 16, 2001.

pulled through a hole in a fixed position water-cooled copper baffle at a constant, preset speed to achieve preferential solidification. This geometry yielded thermal gradients at the liquid/solid interface of about 8 to 10 K/mm. Directional solidification was conducted at withdrawal rates of 7.6, 12.7, 25.4, 50.8, 127, 254, and 508 mm/h to produce aligned regions about 100-mm long; except at the slowest speed, where, due to operating time limits on the equipment, the DS length was about 50 mm.

Compression, fracture toughness, and chemistry and metallography specimens were taken from the aligned region of the DS bars and as-cast rods by wire electro-discharge machining (EDM), where the long axis of the mechanical property samples was parallel to the growth/casting direction. While the major surfaces of the approximately $8 \times 4 \times 4$ mm compression specimens were ground to remove EDM surface damage, the opposing 4 by 4 mm loading surfaces were left in the as–electrodischarge machined condition. The fracture toughness bars, 50-mm long and 6×3 mm in cross section, were machined in accordance to the ASTM-399 bend specimen geometries[12] with the as-cast EDM layers being removed by grinding on emery paper to a finish of 600 grit.

Fracture toughness of the alloys at room temperature was measured in three-point bending in accordance with ASTM E399,[12] with one main exception. The precracks were generated by using the bridge indentation technique[13] instead of cyclic fatigue. The test specimens were loaded at a stroke rate of 0.0033 mm/s on a 24-mm support span. The specimen stability was monitored by either a clip gage, as required by E399, or by a strain gage placed on the compressive face of the specimen.[14] Both methods were adequate for assessing the specimen stability. Three to five valid toughness tests were conducted on specimens from each growth condition with the exception of the alloy DS at 7.6 mm/h, where only two valid results were obtained.

Elevated temperature compressive strength in air was evaluated over three to six orders of magnitude in strain rate between 1200 and 1400 K through a combination of constant velocity and constant load creep testing. Constant velocity testing was conducted in a universal testing machine, where each sample was compressed along its length between two solid SiC push bars at crosshead speeds varying between 8.5×10^{-7} and 1.3×10^{-3} mm/s. The autographically recorded load-time curves were converted to true stresses, strains, and strain rates *via* the offset method in combination with a normalization to the final specimen length and the assumption of constant volume. Constant load compressive creep testing to measure properties in the 10^{-6} to 10^{-8} s^{-1} range was undertaken in lever arm test machines, where deformation was determined as a function of time by measuring the relative positions of the ceramic push bars applying the load. While most creep tests were conducted under a single load, a few specimens were subjected to multiple load conditions. Contraction-time creep data were normalized with respect to the final specimen length and converted into true stresses and strains. The temperature-stress-deformation rate behavior of the Ni-33Al-33Cr-1Mo materials was characterized using the stress and strain rate at 1 pct deformation from each constant velocity test along with the steady-state creep rates and the average true stress from the constant load creep experiments.

Light optical techniques were used to conduct detailed metallographic observations on both the longitudinal and transverse polished samples taken from several as-cast bars and the aligned region of each DS rod. In general, two widely separated samples were taken from the directional solidification portion of each DS rod and each as-cast bar for chemistry. Analysis to determine both major and minor solute metallic elements (Ni, Al, Cr, Mo, *etc.*) was performed by an inductively coupled plasma (ICP) technique, while the concentrations of nitrogen and oxygen were determined by an inert gas fusion method, and the carbon level was measured by the combustion extraction method.

III. RESULTS AND DISCUSSION

A. *Alloy Composition*

The arithmetic averages, standard deviations, as well as the maximum and minimum values for all the elements found by chemical analysis of either the as-cast or DS versions of the Ni-33Al-33Cr-1Mo alloys are reported in Table I. These results summarize the data gathered from duplicate chemistry samples taken from the as-cast bars and DS rods grown at rates ranging from 12.7 to 254 mm/h in addition to single samples from the as-cast bars and DS rods used for the 7.6 and 508 mm/h runs.

Table I(a) indicates that the control of the alloy chemistry for all seven as-cast bars and DS rods was quite good, with the average values for the major elements being close to the intended Ni-33Al-33Cr-1Mo composition. While there is little change between the Mo levels among the as-cast and DS alloys, surprisingly, directional solidification appeared to increase the difference between the maximum and minimum values for both Al and Cr, and thus Ni, over those measured in the as-cast bars. Such changes are, in turn, reflected by the larger standard deviations for the DS rods. The greater variation in the concentration of major elements for the DS materials compared to the initial as-cast alloys is also reflected in the Al/Ni ratios (Table I(a)), which are a measure of stoichiometry in NiAl. While directional solidification slightly reduces the average Al/Ni ratio, this processing increases the range of values compared to those found in the as-cast alloys.

In addition to the desired alloying elements, three metallic (Cu, Fe, Si) and four interstitial (C, N, O, S) impurities were found in both forms of Ni-33Al-33Cr-1Mo (Table I(b)). In terms of the highest concentrations of unintentional alloying elements, the as-cast bars average about 0.05 at. % of C, O, and Si (Table I(b)). While the C distribution appears to be unaffected by processing, the order of magnitude difference in average Si level and factor of 6 decrease in maximum Si content between the as-cast and DS materials suggest that the directional solidification zone refines this impurity. Although the average O content in the as-cast and DS version is unchanged, the factor of 4+ decrease in standard deviation and range indicates that directional solidification homogenizes the O levels.

Table I. Composition and Al/Ni Ratios of As-Cast and DS Ni-33Al-31Cr-1Mo Alloys

(a) Major Elements in Atomic Percent

	As-Cast Alloys				DS Alloys			
	Average	Standard Deviation	Maximum	Minimum	Average	Standard Deviation	Maximum	Minimum
Al	32.99	0.28	33.41	32.43	32.85	0.68	33.71	31.21
Cr	33.33	0.14	33.56	33.08	33.47	0.54	34.90	32.88
Mo	1.03	0.01	1.05	1.00	1.02	0.02	1.04	0.99
Ni	32.51	0.22	32.82	32.22	32.55	0.31	33.02	32.00
Al/Ni	1.02	0.01	1.03	1.00	1.01	0.03	1.05	0.98

(b) Minor Elements in Atomic Parts per Million

	As-Cast Alloys				DS Alloys			
	Average	Standard Deviation	Maximum	Minimum	Average	Standard Deviation	Maximum	Minimum
C	561	96	829	467	658	135	910	527
Cu	29	22	66	4	92	170	627	15
Fe	58	107	390	8	96	163	503	17
N	11	8	20	3	20	5	27	13
O	269	225	679	38	311	46	393	238
S	8	4	13	1	6	3	13	4
Si	511	328	972	33	48	51	150	33

B. *Alloy Microstructure*

The transverse microstructure of as-cast and DS Ni-33Al-33Cr-1Mo are illustrated in Figure 1, where for completeness each bar/rod is identified by its actual composition. Casting of the alloy into a Cu-chill mold produced NiAl dendrites (starlike and globule regions) scattered among grains containing both NiAl and Cr(Mo) in basically a pearlitic type pattern (Figure 1(a)). Directional solidification at 7.6 and 12.7 mm/h yielded millimeter-diameter planar eutectic grains consisting of parallel, micron-thick Cr(Mo) and NiAl plates delineated by sharp boundaries. While only plates were seen after growth at 12.7 mm/h, a few regions (Figure 1(b)) in the rod grown at 7.6 mm/h contained Cr(Mo) fibers in addition to plates. Directional solidification rates at and above 25.4 mm/h lead to ~200-μm diameter cells enclosed by intercellular regions, where each cell contains thin lamella in a radial pattern (Figures 1(c) through (f)), while thicker plates exist in the intercellular regions. As the directional solidification rate was increased from 25.4 mm/h (Figure 1(c)) to 50.8 mm/h (Figure 1(d)) to 127 mm/h (Figure 1(e)) to 254 mm/h (Figure 1(f)), the intercellular regions became more prominent with coarser structures, while the lamella within the cells became refined.

Examples of the longitudinal microstructure after DS are given in Figure 2, with the analyzed composition for each DS rod used for identification. Growth at the two slowest growth rates of 7.6 and 12.7 mm/h, where planar eutectic grains are formed, produced a longitudinal morphology (Figure 2(a)) consisting of millimeters-long groups of parallel plates, which appear to lie in all orientations. At faster growth rates up to 254 mm/h, where cells are found, the lamella within the millimeter long cells tend to align with the growth direction (Figures 2(b) through (f)). Within the intercellular regions, however, the morphology of the Cr(Mo) and NiAl plates becomes irregular with changes in thickness and orientation occurring. While the Cr(Mo) forms bands, which generally bridge the intercellular regions at growth rates of 25.4 and 50.8 mm/h (Figures 2(b) and (c)), at faster rates, examples of isolated squat plates/blocks of Cr(Mo) in a NiAl matrix start to appear (Figures 2(d) through (f)).

Growth at the fastest rate (508 mm/h) appears to have completely changed the morphology in DS Ni-33Al-33Cr-1Mo from a basically lammellar structure to a two-phase particulate/short fiber structure (Figure 3). Although both transverse (Figure 3(a)) and longitudinal (Figures 3(b) and (c)) sections indicated that the structure is still cellular in nature, the intercellular regions consist of micron-sized Cr(Mo) particles/rods within an NiAl matrix, while the cell interiors contain a uniform dispersion of submicron diameter Cr(Mo) particles or short fibers within the matrix (Figures 3(a) and (c)).

In spite of some differences in chemistry among the DS rods (Table I), no third phases were found nor was there any evidence of NiAl or Cr(Mo) dendrites in Ni-33Al-33Cr-1Mo DS rates ranging from 7.6 to 508 mm/h (Figures 1(b) through (f), 2, and 3). This complete absence of dendrites agrees with the behavior found in the Ni-33Al-31Cr-3Mo eutectic after being DS at the same rates.[4,15] While generally similar structures are found in both DS Ni-33Al-33Cr-1Mo and Ni-33Al-31Cr-3Mo, differences do exist. In particular, at the slower two growth rates (7.6 and 12.7 mm/h, where intercellular regions are not formed in either alloy), the lamella tend to align with the DS growth axis in the 3Mo version[4,15] but not in the 1Mo alloy (Figure 2(a)). After directional solidification between 25.4 to 254 mm/h, the cell interiors and intercellular regions for both eutectic compositions appear basically alike with the exception of the intercellular areas in the rods grown at 254 mm/h, where Cr(Mo) forms well-defined lamella in DS NiAl-31Cr-3Mo[4,15] but not in DS Ni-33Al-1Mo (Figure 1(f)). The most striking difference between the Mo-rich and Mo-poor eutectics exists after DS at 508 mm/h. In this case, the cell interior and intercellular regions of Ni-33Al-33Cr-1Mo contain discrete second-phase particles/rods of Cr(Mo) in an NiAl matrix (Figure 3), whereas a

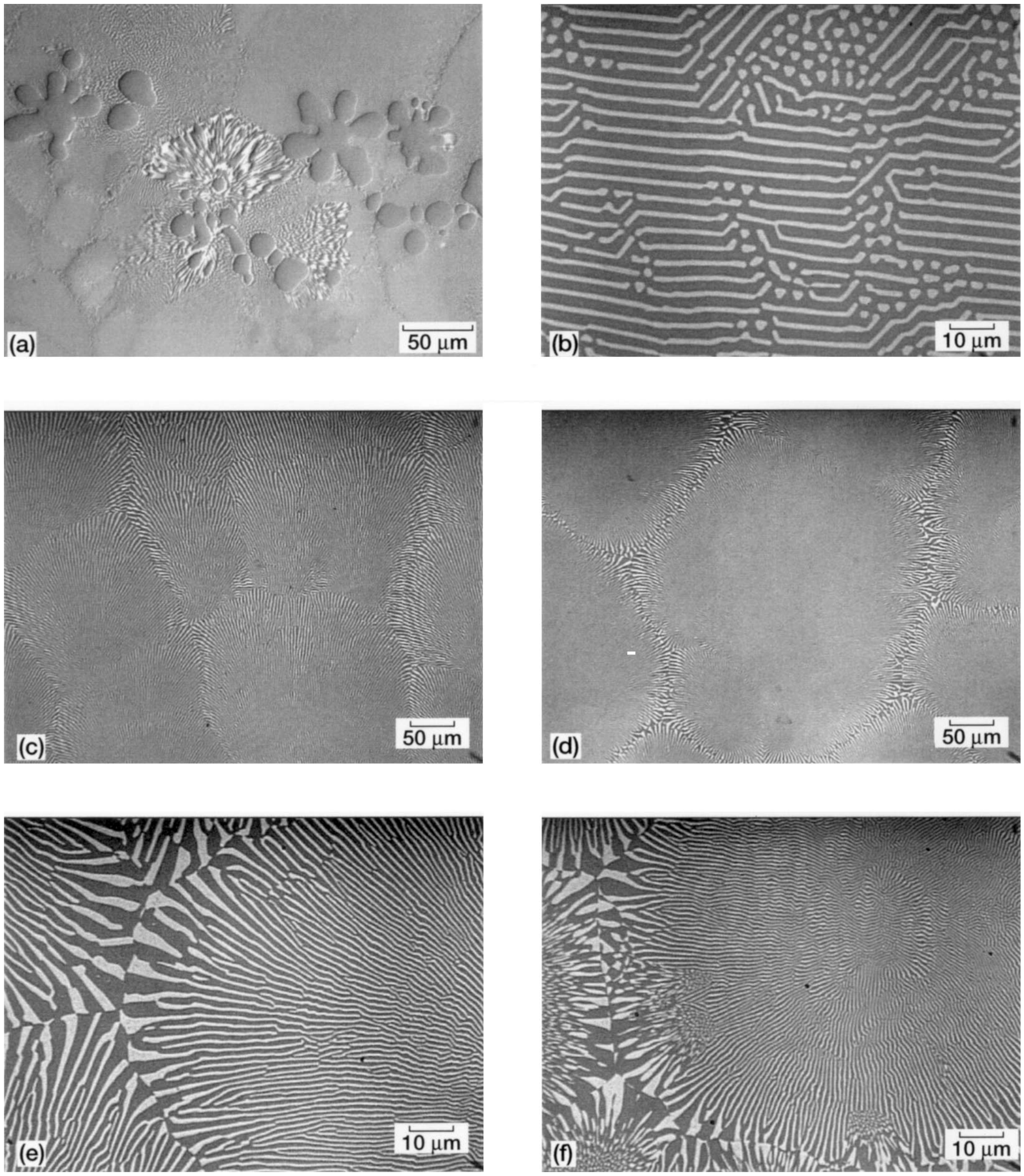

Fig. 1—Light optical unetched microstructure of transverse sections of the as-cast and DS Ni-33Al-33Cr-1Mo eutectic: (*a*) as-cast Ni-33.1Al-33.3Cr-1.03Mo, (*b*) Ni-33.0Al-33.6Cr-1.03Mo DS at 7.6 mm/h, (*c*) Ni-33.4Al-33.1Cr-1.01Mo DS at 25.4 mm/h, (*d*) Ni-33.7Al-33.1Cr-1.00Mo DS at 50.8 mm/h, (*e*) Ni-32.6Al-33.4Cr-1.04Mo DS at 127 mm/h, and (*f*) Ni-32.7Al-33.3Cr-1.02Mo DS at 254 mm/h.

lamellar structure is essentially retained throughout DS Ni-33Al-31Cr-3Mo.[4,15]

At least two other studies involving directional solidification of Ni-33Al-33Cr-1Mo have been undertaken. Cline *et al.*[16] used a Bridgman technique to directionally solidify NiAl-32.4Cr-1Mo at 12.7 mm/h, and they also obtained lamellar eutectic grains with well-defined boundaries, which agrees with Figure 2(a). While growth at or exceeding 25.4 mm/h produced intercellular regions in the present study (Figures 1 and 2), Yang *et al.*[3] were able to grow planner eutectic grains (Figure 1(b)) at both 50 and 100 mm/h through an edge-defined film-fed growth (EDFG) technique. Presumably, EDFG with its much greater thermal gradient through the Ni-33Al-33Cr-1Mo liquid/solid interface allows more prefect structures to be grown than does the Bridgman technique.

C. *Mechanical Properties*

1. *Fracture toughness*

The majority of the fracture toughness specimens exhibited either unstable crack extension or multiple, unstable crack extensions followed by crack arrests, implying little in the way of ductility. For some specimens, measurement of the precrack length was difficult due to the microstructure (Figures 1 through 3); however, heat tinting at 983 K for 1 hour in air was generally sufficient for identifying the precracks.

One of the main difficulties in measuring fracture toughness was the generation of an acceptable precrack. Because the DS Ni-33Al-33Cr-1Mo exhibited a relatively low elastic modulus and large fracture toughness, the precracking fixture and specimen parameters outlined in PS070,[14] which

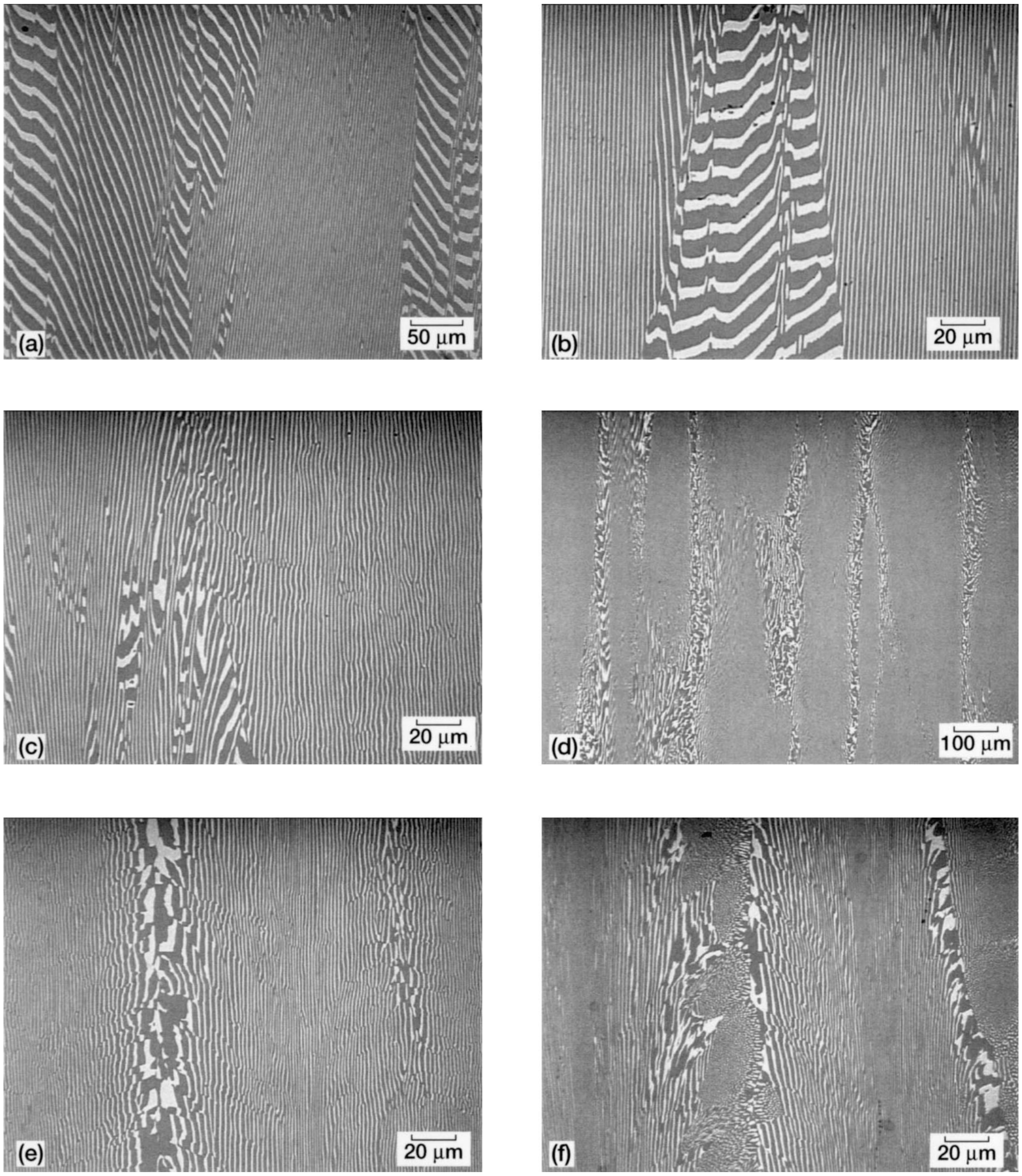

Fig. 2—Light optical unetched microstructure of longitudinal sections of the DS Ni-33Al-33Cr-1Mo eutectic: (*a*) Ni-31.8Al-34.4Cr-1.02Mo DS at 12.7 mm/h, (*b*) Ni-33.4Al-33.1Cr-1.01Mo DS at 25.4 mm/h, (*c*) Ni-33.7Al-33.1Cr-1.00Mo DS at 50.8 mm/h, (*d*) and (*e*) Ni-32.6Al-33.4Cr-1.04Mo DS at 127 mm/h, and (*f*) Ni-32.7Al-33.3Cr-1.02Mo DS at 254 mm/h. The growth direction is vertical.

are appropriate for ceramics materials, tended to generate cracks of excessive length. Shorter precracks were attained by using a narrow bridge span (~2 mm) and by sharpening the starter notch, which was cut by EDM, with a razor blade and diamond paste.

The average room-temperature toughness values for DS Ni-33Al-33Cr-1Mo are illustrated as a function of growth rate in Figure 4. For DS rate ranging from 7.6 to 127 mm/h, the materials exhibit a plateau of ~16 MPa$\sqrt{m}$. However, at faster directional solidification rates, the toughness falls off significantly, where the value for Ni-33Al-33Cr-1Mo grown at 254 and 508 mm/h is essentially the same as that for NiAl.[17] The relatively high toughness of 16 MPa $\sqrt{m}$ is in good agreement with the value of 17.3 MPa $\sqrt{m}$ obtained in Ni-33Al-33Cr-1Mo by Yang *et al.*[3]

The 16 MPa$\sqrt{m}$ value for Ni-33Al-33Cr-1Mo DS between 7.6 and 127 mm/h (Figure 4) agrees with the measurements for DS Ni-33Al-31Cr-3Mo,[4] where an ~16 MPa$\sqrt{m}$ plateau exists for material DS between 12.7 and 508 mm/h. The most striking difference in toughness between these two Mo-modified NiAl-34Cr alloys is the behavior of the materials grown at the fastest rates. While the 3Mo eutectic retains a 16 MPa$\sqrt{m}$ toughness for material grown at 254 and 508 mm/h, the 1Mo eutectic displays toughness of only about 7 MPa$\sqrt{m}$ after directional solidification at these rates (Figure 4). At least for the fastest growth rate (508 mm/h), the loss of toughness can probably be ascribed to changes in the microstructure, where Ni-33Al-31Cr-3Mo has retained its lamellar-type microstructure,[4] while the structure of Ni-33Al-33Cr-1Mo was reduced to Cr(Mo) particles/short fibers in a NiAl matrix (Figure 3). A partial transformation to Cr(Mo) particles/short fibers also

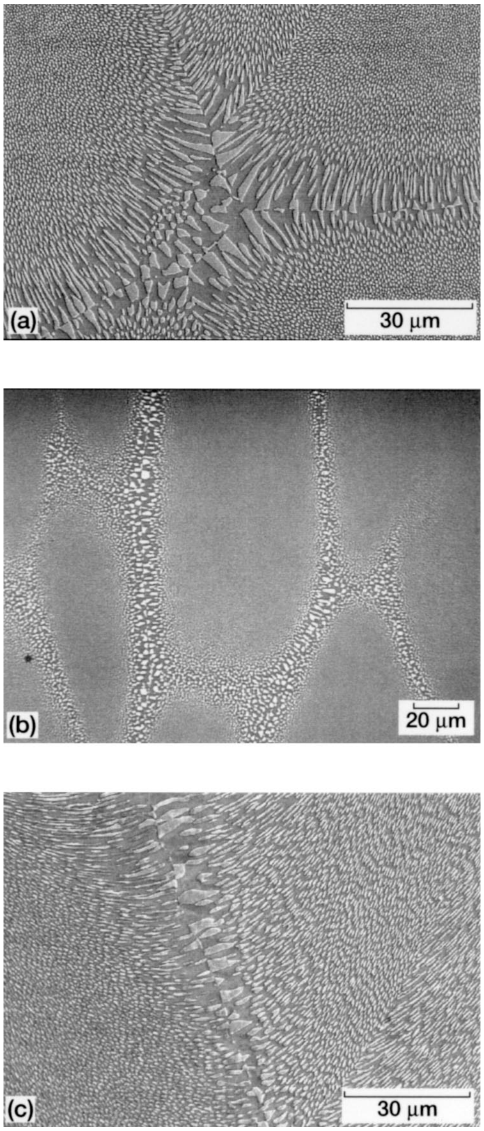

Fig. 3—Light optical unetched microstructure of a (*a*) transverse section and (*b*) and (*c*) longitudinal sections of Ni-32.9Al-33.3Cr-1.02Mo DS at 508 mm/h. The growth direction is vertical in parts (b) and (c).

seems to be occurring in the 1Mo version directional solidification at 254 mm/h (Figure 2(f)), and this could be the reason for the large loss in toughness compared to those for the slower growth rates (Figure 4).

Based on some recent work of Misra *et al.*,[18] a high interstitial element content could be another possible reason for the low toughness of Ni-Al-33Cr-1Mo DS at fast rates. Their study of DS NiAl-34Cr indicated that C, N, and O content can affect the toughness. Particular alloys with about 370 appm C, 450 appm N, and 230 appm O had a toughness of about 10 MPa$\sqrt{m}$, whereas purer eutectics with 140 appm C, 50 appm N, and 20 appm O exhibited an ~20 MPa$\sqrt{m}$ toughness. Neglecting any possible gettering effects due to the substitution of some Mo for Cr, high interstitial contents do not appear to be the reason for low toughness in DS Ni-33Al-33Cr-1Mo. As presented in Table I, all the current DS Ni-33Al-33Cr-1Mo rods contained relatively high concentrations of C (~650 appm) and O (~310 appm) coupled with a low N level (~20 appm); furthermore,

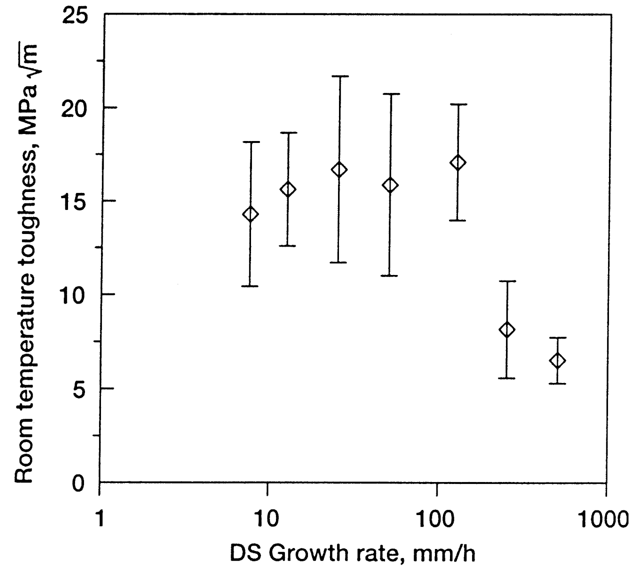

Fig. 4—Room-temperature fracture toughness as a function of growth rate for DS Ni-33Al-33Cr-1Mo, where error bars indicate the plus or minus two standard deviation limits.

DS Ni-33Al-31Cr-3Mo possesses good toughness values along with approximately 600 appm C, 35 appm N, and 350 appm O.[4] Therefore, interstitial element content, alone, does not appear to be a controlling factor for toughness in Mo-modified NiAl-Cr alloys.

D. *Elevated Temperature Compressive Properties*

1. *Stress-strain and creep behavior*

Examples of the stress-strain diagrams generated by 1300 and 1400 K constant velocity testing are presented in Figure 5 for as-cast (parts (a) and (b)) and DS Ni-33Al-33Cr-1Mo (parts (c) through (f)). As portrayed in Figure 5, the stress-strain curves display work hardening during the initial 1 pct strain followed by continued deformation at a more or less constant stress for the majority of the material/test conditions. However, instances of strain hardening (Figure 5(a)) and strain softening (Figure 5(c)) were also observed. Figure 5 illustrates that (1) at each test temperature, the strength of the material decreases with a decreasing strain rate; and (2) at common deformation rates, the strength of as-cast (Figures 5(a) and (b)), DS at 127 mm/h (Figures 5(c) and (d)), and DS at 508 mm/h (Figures 5(e) and (f)) is greater at 1300 K than at 1400 K. The benefit of elevated temperature strength due to directional solidification can be seen in the slower strain rate results, where, for example, at 1300 K, the as-cast material (Figure 5(a)) is weaker than either DS version (Figures 5(c) and (e)). Similar behavior exists at 1400 K (Figures 5(b), (d), and (f)). Comparison of the properties of the alloy grown at 127 mm/h (Figures 5(c) and (d)) to those of Ni-33Al-33Cr-1Mo grown at 508 mm/h (Figures 5(e) and (f)) demonstrates that the rate of directional solidification can affect strength, where a faster growth rate leads to a weaker material.

Typical creep curves from constant load testing of Ni-33Al-33Cr-1Mo between 1200 and 1400 K are given in Figure 6. Both as-cast (Figure 6(a)) and DS Ni-33Al-33Cr-1Mo (Figure 6(b)) displayed normal creep behavior, where

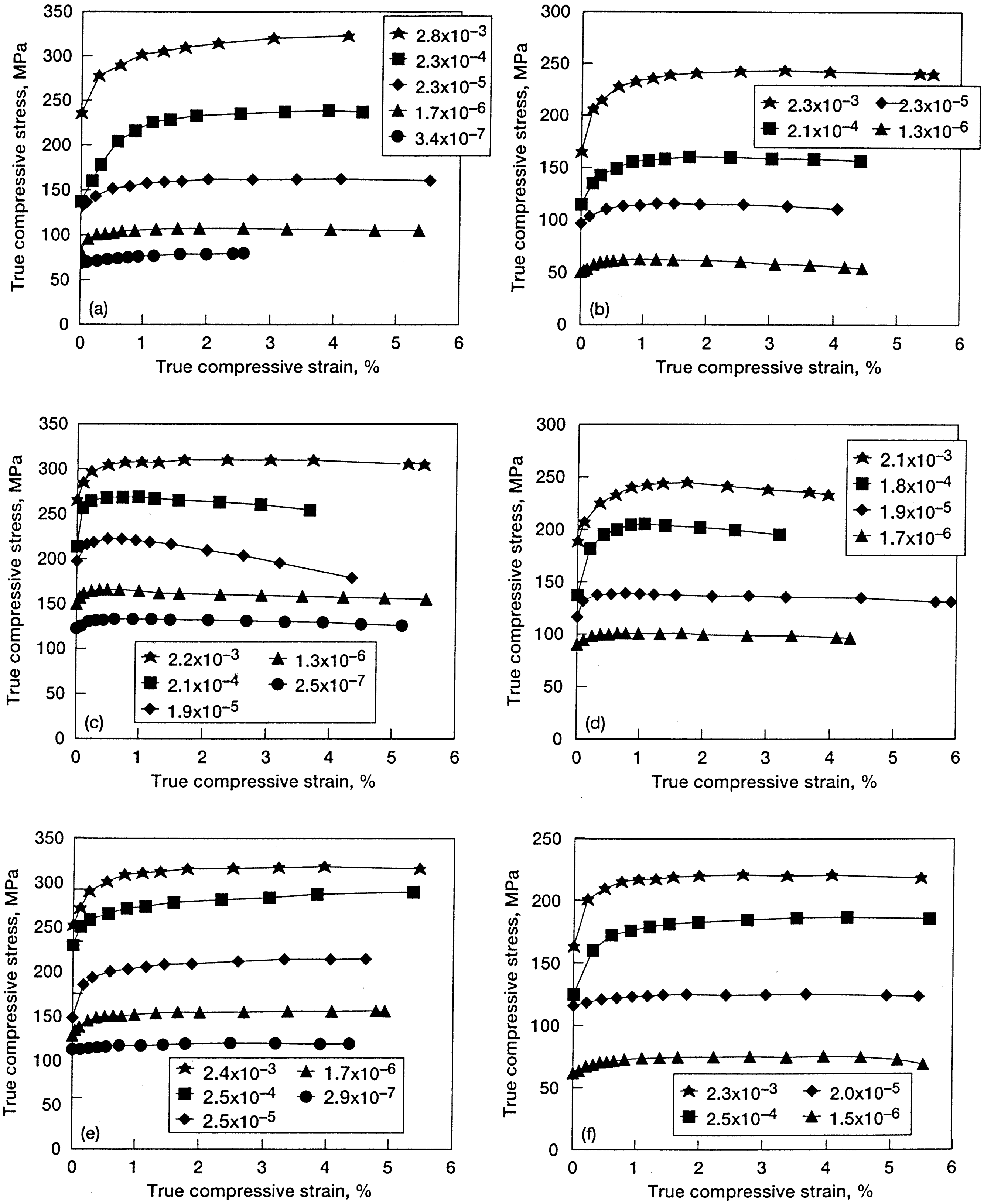

Fig. 5—True compressive stress-strain curves for Ni-33Al-33Cr-1Mo as a function of nominal strain rate: as-cast at (*a*) 1300 K and (*b*) 1400 K; DS at 127 mm/h at (*c*) 1300 K and (*d*) 1400 K; and DS at 508 mm/h at (*e*) 1300 K and (*f*) 1400 K.

the transient regime was supplanted to steady state, even when multiple constant load conditions were used: the 1200 K test in Figure 6(a); and the 1400 K and one of the 1200 K tests in Figure 6(b). Visual contrasting of the creep curves for the two forms of Ni-33Al-33Cr-1Mo again demonstrates the strength advantage due to DS; for example, about 2 pct

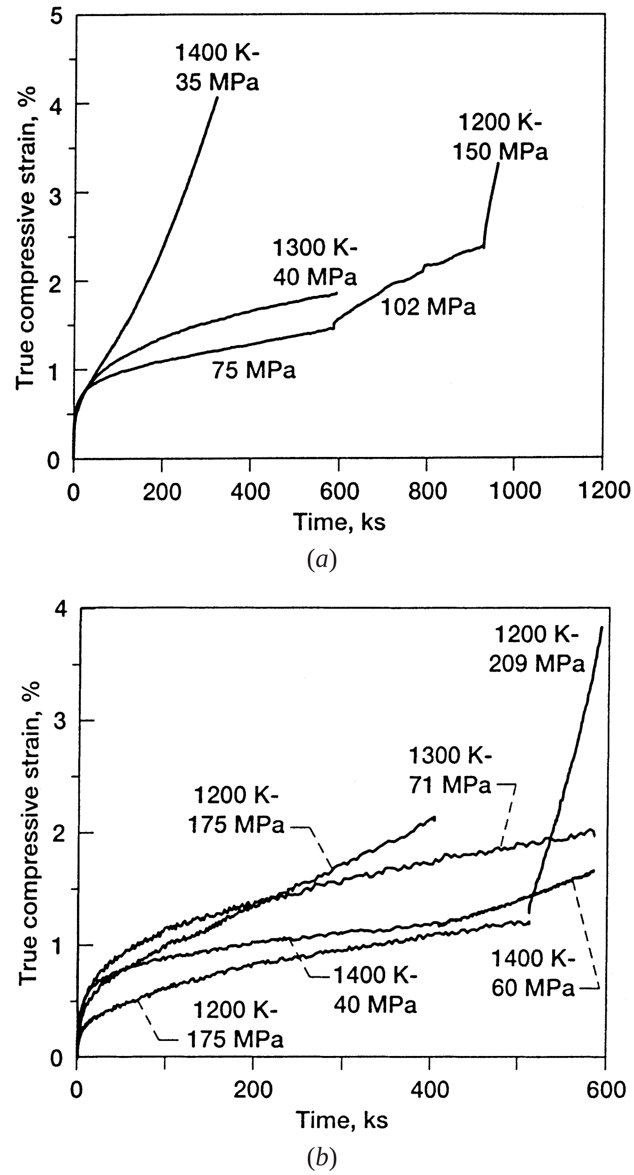

Fig. 6—True compressive creep curves for Ni-33Al-33Cr-1Mo tested under various engineering stress conditions: (*a*) as-cast and (*b*) DS at 25.4 mm/h.

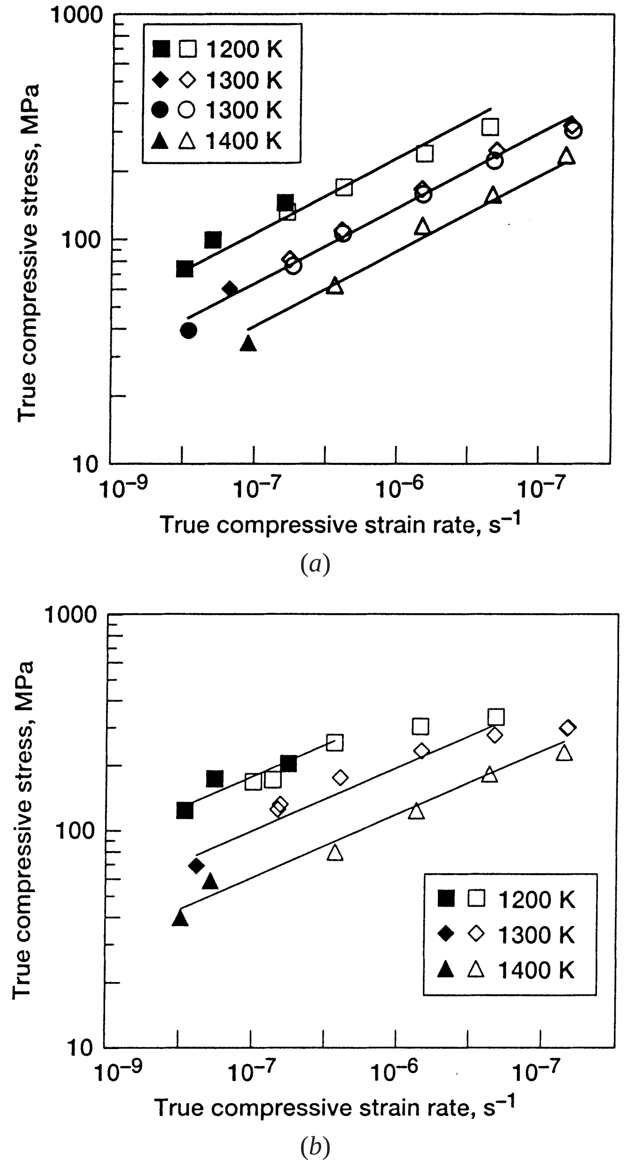

Fig. 7—True compressive flow stress-strain rate-temperature behavior of Ni-33Al-33Cr-1Mo: (*a*) as-cast and (*b*) DS at 25.4 mm/h. Open symbols are data from constant velocity testing, while solid symbols represent results from creep testing.

deformation occurred in ~600 ks at 1300 K in the as-cast alloy under an engineering stress of 40 MPa (Figure 6(a)), while the DS material required a 71 MPa stress (Figure 6(b)).

2. *Flow stress-strain rate-temperature behavior*

Figure 7 illustrates two sets of flow stress-strain rate-temperature data for Ni-33Al-33Cr-1Mo, where the results from constant velocity testing are shown as open symbols, and the values from creep tests are given as solid symbols. The 1300 K data in Figure 7(a) show that the properties of two as-cast bars (diamonds and circles) are nearly identical, and the 1200 K data in Figures 7(a) and (b) demonstrate that both constant velocity and constant load creep testing yield equivalent strength levels. In general, the majority of the gathered data could be described by either a temperature-compensated exponential or power law, with the exponential law being better at faster strain rates/lower temperatures and the power law more appropriate at slower strain rates/higher temperatures. The format and curves in Figure 7 illustrate the results from temperature-compensated power-law fits (Eq. [1]) of the data, where

$$\dot{\varepsilon} = A\sigma^n \exp(-Q/(RT)) \qquad [1]$$

where $\dot{\varepsilon}$ is the strain rate in s^{-1}, A is a constant, σ is the stress in MPa, Q is the activation energy, R is the universal gas constant, and T is the absolute temperature. The deformation parameters from temperature-compensated power-law fitting by linear regression analysis of the as-cast alloy and Ni-33Al-33Cr-1Mo DS at rates from 12.7 to 254 mm/h are given in Table II(a). The elevated temperature properties for the alloy DS at either 7.6 or 508 mm/h could only be reasonably described by a temperature-compensated exponential law (Eq. [2]):

$$\dot{\varepsilon} = A \exp(C\sigma) \exp(-Q/RT) \qquad [2]$$

where C is the stress constant. The results for these latter

Table II. Descriptions of the Flow Stress-Strain Rate Properties for Ni-33Al-33Cr-1Mo

(a) Temperature-Compensated Power Law

Identification	Temperature (K)	Strain Rate Regime (s^{-1})	A (s^{-1})	n	Q (kJ/mol)	R_d^2	δ_n	δ_Q (kJ/mol)
As cast	1200	10^{-8} to 10^{-4}	1.69×10^{-2}	6.02	−400.3	0.979	0.19	25.3
	1300	10^{-8} to 10^{-3}						
	1400	10^{-7} to 10^{-3}						
DS at 12.7 mm/h	1200	10^{-8} to 10^{-4}	1.25×10^{-5}	7.74	−431.3	0.952	0.44	45.9
	1300	10^{-8} to 10^{-3}						
	1400	10^{-8} to 10^{-3}						
DS at 25.4 mm/h	1200	10^{-8} to 10^{-6}	0.844	6.82	−511.5	0.957	0.36	35.9
	1300	10^{-8} to 10^{-4}						
	1400	10^{-8} to 10^{-3}						
DS at 50.8 mm/h	1200	10^{-8} to 10^{-5}	5.57×10^{-5}	7.82	−465.4	0.957	0.44	41.6
	1300	10^{-8} to 10^{-4}						
	1400	10^{-6} to 10^{-3}						
DS at 127 mm/h	1200	10^{-7} to 10^{-4}	1.35×10^{-9}	9.00	−411.7	0.948	0.68	40.1
	1300	10^{-7} to 10^{-3}						
	1400	10^{-6} to 10^{-3}						
DS at 254 mm/h	1200	10^{-7} to 10^{-4}	1.39×10^{-8}	8.60	−412.4	0.976	0.42	33.6
	1300	10^{-8} to 10^{-4}						
	1400	10^{-6} to 10^{-3}						

(b) Temperature-Compensated Exponential Law

Identification	Temperature (K)	Strain Rate Regime (s^{-1})	B (s^{-1})	C	Q (kJ/mol)	R_d^2	δ_c	δ_Q (kJ/mol)
DS at 7.6 mm/h	1200	10^{-7} to 10^{-6}	2.28×10^{11}	0.0491	−494.9	0.977	0.003	36.3
	1300	10^{-7} to 10^{-3}						
	1400	10^{-6} to 10^{-3}						
DS at 508 mm/h	1200	10^{-7} to 10^{-4}	3.03×10^{6}	0.0515	−376.0	0.993	0.0013	14.9
	1300	10^{-7} to 10^{-3}						
	1400	10^{-6} to 10^{-3}						

two conditions are presented in Table II(b). For completeness, Table II lists the temperature and approximate strain rate range of the data used in each fit, the coefficient of determination for the fit (R_d^2), and the standard deviations for the stress exponent (δ_n), stress constant (δ_C), and activation energy (δ_Q).

Although the relatively large range in activation energies and power-law stress exponents in Table II(a) would suggest a wide variance in behavior among the various DS growth rates, summary plots (Figure 8) of the flow stress-strain rate data as a function of growth rate indicated that this is not the case. With the use of a semilog format to separate the data, it can be seen that Ni-33Al-33Cr-1Mo DS at rates from 12.7 to 254 mm/h appears to possess nominally equal strengths at 1200 K (Figure 8(a)) 1300 K (Figure 8(b)), and 1400 K (Figure 8(c)). Furthermore, the deformation resistance of the alloys DS between 12.7 and 254 mm/h is much greater than that exhibited by the as-cast version except at the fastest strain rates. While Ni-33Al-33Cr-1Mo DS at intermediate rates is strong, the eutectic grown at 7.6 and 508 mm/h consistently displays inferior strength levels (Figure 8). In fact, Ni-33Al-33Cr-1Mo grown at the fastest and slowest rate exhibits 1200 to 1400 K slow strain rate strengths, which are only slightly greater than those for the as-cast alloy.

Statistical testing using Eq. [1] in combination with a dummy variable was applied to determine if differences in properties existed among the alloys DS at rates from 12.7 to 254 mm/h. This examination began by contrasting the flow stress-strain rate-temperature results for the 25.4 and 50.8 mm/h versions. As no differences were found, these two sets of data were joined and tested against the properties of the alloy grown at 127 mm/h. This procedure then was applied to the data for the 254 mm/h alloy and finally to the 12.7 mm/h material. Use of this dummy variable approach indicated that Ni-33Al-33Cr-1Mo DS at 25.4, 50.8, 125, and 254 mm/h possessed equivalent 1200 to 1400 K deformation behavior, which can be described with a single stress exponent and activation energy by

$$\dot{\varepsilon} = 2.35 \times 10^{-4}\ \sigma^{7.58} \exp(-464.1/(RT)) \qquad [3]$$

where $R_d^2 = 0.947$, $\delta_n = 0.25$, and $\delta_Q = 21.0$ kJ/mol. The relatively high coefficient of determination and the visual presentation of the data along with the predictions of Eq. [3] in Figure 9 strongly suggest that the strength properties of DS Ni-33Al-33Cr-1Mo are not dependent on growth rates between 25.4 and 254 mm/h.

While it is clear from Figure 8 that the strength properties of as-cast Ni-33Al-33Cr-1Mo and the versions DS at 7.6 or 508 mm/h are weaker than those DS between 25.4 and 254 mm/h, the deformation behavior of the 12.7 mm/h material visually appears to be equivalent to this latter group (Figure 8). However, extension of the dummy variable approach to the 12.7 mm/h results indicated that this growth rate resulted in properties that were slightly weaker than that described by Eq. [3].

3. *Strength comparisons*

A few measurements of the slow plastic deformation strength of DS NiAl-34Cr and DS Ni-33Al-33Cr-1Mo at or near 1300 K have been reported in the literature. Some of these results are shown in Figure 10(a), where Pollock and

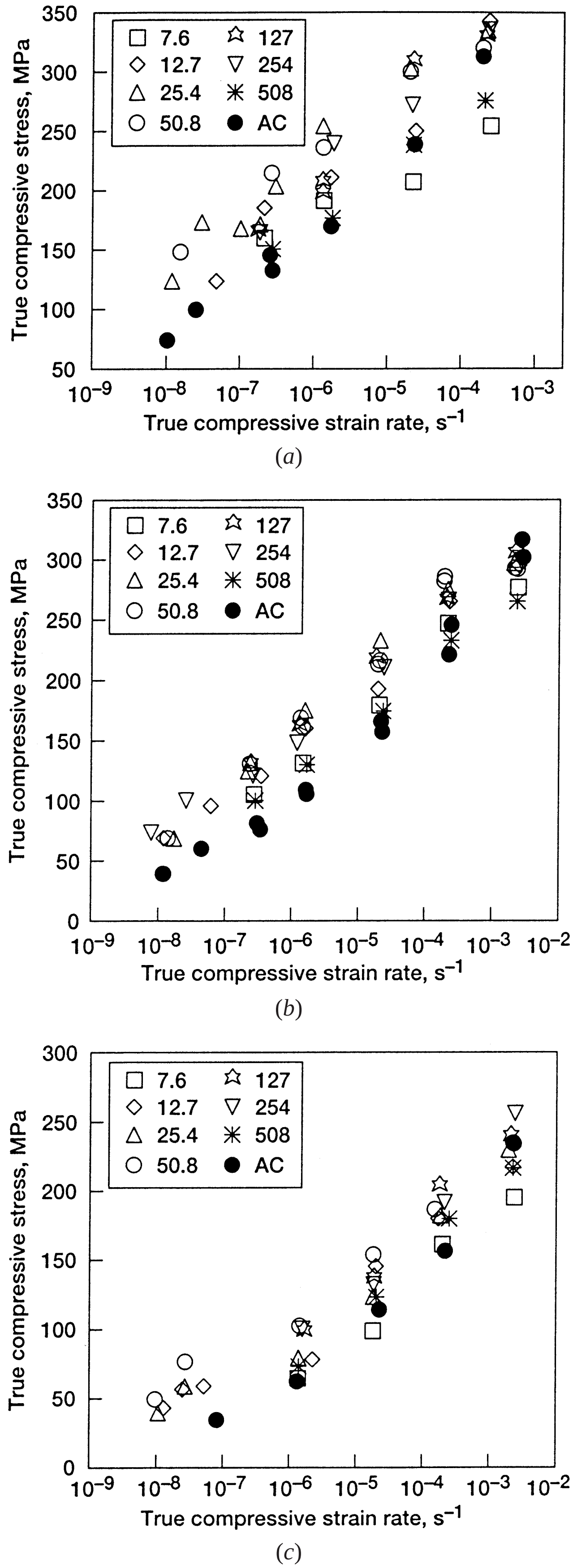

Fig. 8—True compressive flow stress-strain rate behavior of Ni-33Al-33Cr-1Mo as a function of growth rate in mm/h at (*a*) 1200 K, (*b*) 1300 K, and (*c*) 1400 K, where AC signifies the as-cast alloy.

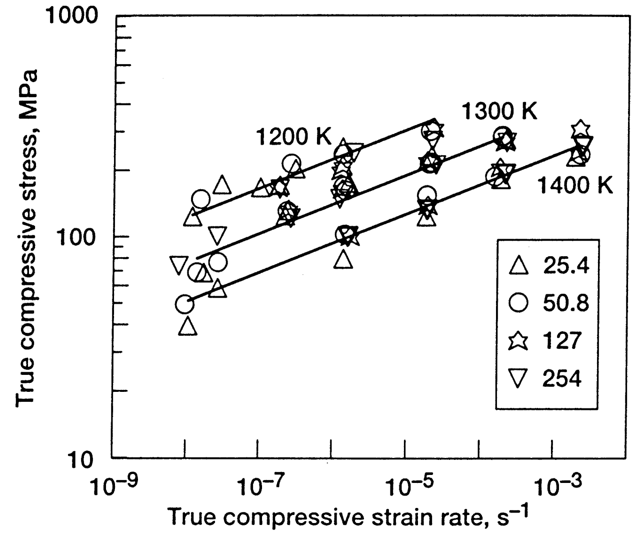

Fig. 9—True compressive flow stress-strain rate-temperature behavior of Ni-33Al-33Cr-1Mo DS at 25.4, 50.8, 127, and 254 mm/h.

Kolluru's 1273 K data points for DS Ni-31.3Al-35.6Cr and DS Ni-33.5Al-32.2Cr-1.1Mo[19] are contrasted with the curves describing Johnson *et al.*'s 1300 K strength for DS NiAl-33.4Cr-0.1Zr[2] and the current 1300 K properties for DS Ni-33Al-33Cr-1Mo (Eq. [3]). Taken together, these data reveal that the elevated temperature properties of both DS NiAl-34Cr and NiAl-33Cr-1Mo are reproducible and essentially the same.

Preliminary elevated temperature compression test results for Ni-33Al-31Cr-3Mo DS at rates between 7.6 and 508 mm/h has been presented,[4] and the resultant flow stress-strain rate-temperature results are similar to those shown in Figure 8. Since publication of this work, additional testing of DS Ni-33Al-31Cr-3Mo has been undertaken,[20] and it has revealed that the flow stress-strain rate-temperature behavior of all the growth conditions, with one exception,* can be described by

$$\dot{\varepsilon} = 1000\sigma^{4.99} \exp(-487.3/(RT)) \qquad [4]$$

*Ni-33Al-31Cr-3Mo DS at 25.4 mm/h was a bit stronger than the other growth rates, but its properties can be described by Eq. [4], where the pre-exponential term is 519 instead of 1000; thus, the 25.4 mm/h version possesses a ~14 pct strength advantage over the other growth rates.

The strength properties of both 1 Mo- and 3 Mo-modified NiAl-34Cr eutectic can now be estimated through Eqs. [3] and [4], and this comparison is made in Figure 10(b). While both DS alloys possess about the same strength levels at each temperature, it is clear that the long-term characteristics of the 3 Mo version are inferior. Because the activation energies for deformation are almost identical (Eqs. [3] and [4]), the relative weakness of Ni-33Al-31Cr-3Mo results from its lower stress exponent (4.99, Eq. [4]) as opposed to the higher value (7.58, Eq. [3]) for DS Ni-33Al-33Cr-1Mo.

The elevated temperature compressive properties of a very high Mo content DS NiAl-Cr eutectic (Ni-33Al-28Cr-6Mo) have also been measured.[2] The behavior of this material is compared to that for DS Ni-33Al-33Cr-1Mo in Figure 10(c)), where visual inspection shows that increasing the Mo content from 1 to 6 at. pct will improve the 1200 to 1400 K strength. However, the benefit appears to be, at best, small in the slower strain rate regimes.

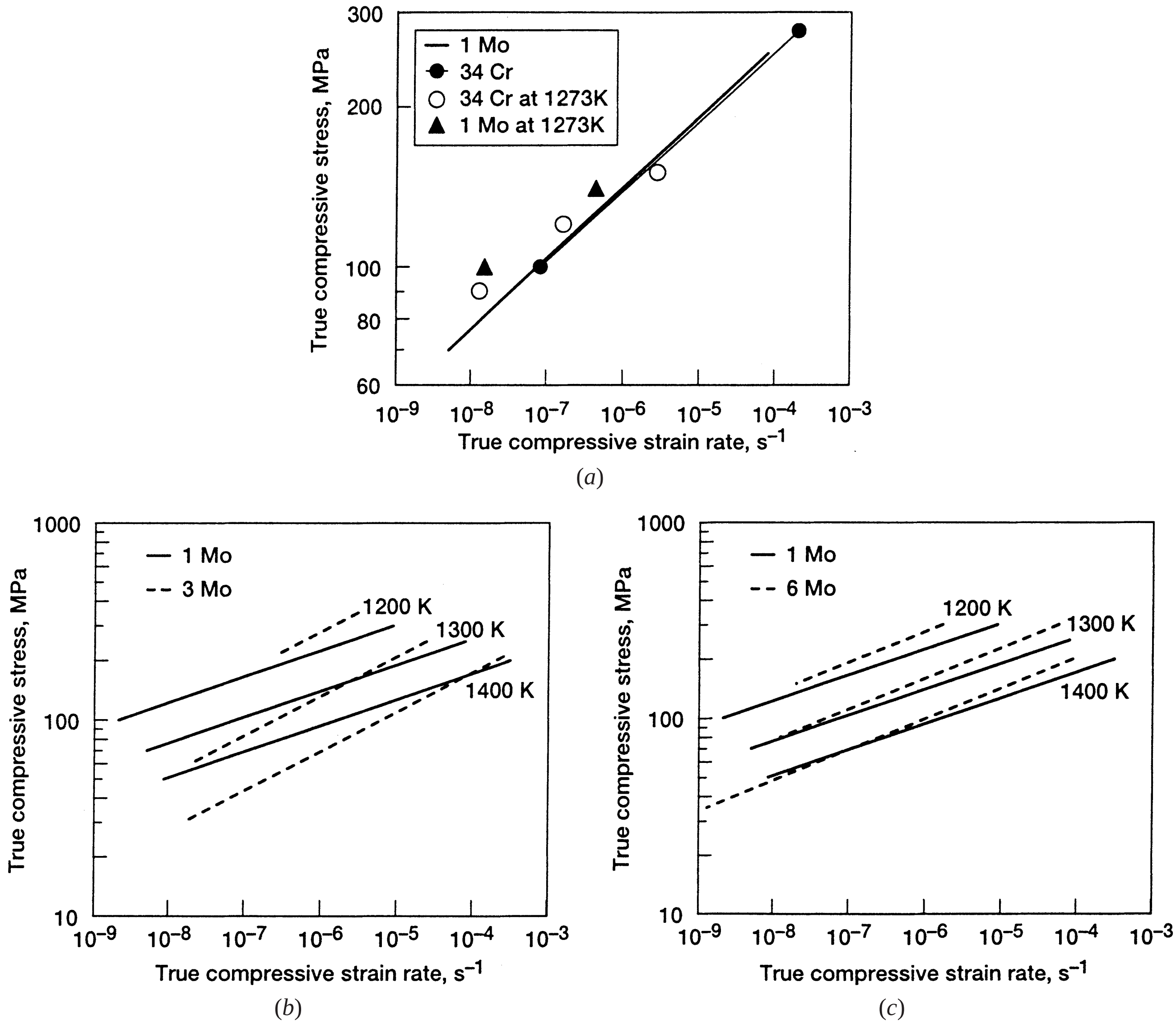

Fig. 10—Comparison of the elevated temperature deformation properties of (*a*) DS Ni-33Al-33Cr-1 Mo and NiAl-34Cr at nominally 1300 K,[2,19] (*b*) DS Ni-33Al-33Cr-1 Mo and Ni-33Al-31Cr-3Mo, (Refs. 4 and 20) between 1200 and 1400 K, and (*c*) DS Ni-33Al-33Cr-1Mo and Ni-33Al-28Cr-6Mo[2] between 1200 and 1400 K. For identification purposes, in part (a), the curve illustrating Johnson *et al.*'s[2] 1300 K strength of Ni-33Al-34Cr-1Zr is anchored by solid circles, while the open circles and solid triangles denote Pollock and Kolluru's 1273 K data for DS Ni-31.3Al-35.6Cr and Ni-33.5Al-32.2Cr-1.1Mo, respectively.

From the elevated temperature strength results in Figure 10, there appears to be little reason to replace Cr with Mo in NiAl-34Cr eutectics. Furthermore, as the 1200 to 1400 K properties of DS Ni-33Al-33Cr-1Mo are not dependent on growth rates ranging from 25.4 to 254 mm/h (Figure 9), changes in microstructural parameters, such as a refinement in interlamellar spacing, cell diameters, and intercellular regions (Figures 1(b) through (f), and 2(b) through (f)), are either unimportant or act in a manner to counterbalance each other. However, comparison to the previous study by Yang *et al.*[3] reveals that microstructure still could be important. Their planar eutectic NiAl-33Cr-1Mo produced by the EDFG technique displayed relatively high ultimate tensile strengths (UTS) at elevated temperature, which are given in Table III along with their UTS results for DS NiAl-34Cr. Both sets of data were regression fitted as a linear function of temperature, and the resultant equations were then used to predict strength levels at 1200, 1300, and 1400 K. The predictions along with the estimated compressive strengths for our DS Ni-33Al-33Cr-1Mo and Johnson *et al.*'s[2] NiAl-34Cr are also shown in Table III. Comparison of the predicted values shows reasonable agreement among Yang *et al.*'s and Johnson *et al.*'s NiAl-34Cr results and those for the current Ni-33Al-33Cr-1Mo. But the strengths of these alloys are clearly inferior to the expectations for Yang *et al.*'s DS Ni-33Al-33Cr-1Mo. If, as is shown in Figure 10(a), the substitution of 1 Mo for 1 Cr is unimportant, then the better properties of Yang *et al.*'s Ni-33Al-33Cr-1Mo must be due to a "better" microstructure.

While extrapolations of fast test results into the creep regime is problematic, the well-behaved characteristics of DS Ni-33Al-33Cr-1Mo (Figures 7 and 9) suggest that good strengths at fast strain rates can translate into good strengths at slow deformation rates. Thus, work to define a "good" microstructure for high-temperature strength in DS NiAl-Cr eutectics is needed.

Table III. Measured and Predicted UTSs ($\dot{\varepsilon} = 5 \times 10^{-4}$ s^{-1}) for DS NiAl-34 Cr and DS Ni-33Al-33Cr-1Mo as a Function of Temperature

Alloy	Temperature (K)	Measured UTS (MPa)	Predicted UTS (MPa)	Reference
NiAl-34Cr	1073	370	—	Yang *et al.*[3]
	1273	296	—	
	1473	195	—	
	1200	—	342	
	1300	—	299	
	1400	—	255	
NiAl-34Cr	1300	—	309*	Johnson *et al.*[2]
NiAl-33Cr-1Mo	1144	546	—	Yang *et al.*[3]
	1255	418	—	
	1366	348	—	
	1200	—	487	
	1300	—	397	
	1400	—	308	
Ni-33Al-33Cr-1Mo	1200	—	350**	this study
	1300	—	319	
	1400	—	213	

*Compressive flow stress.
**Estimated from Fig. 8(a).

4. *Strengthening mechanisms in DS NiAl-Cr based eutectics*

According to Cline and Walter,[6] the growth axis of both NiAl and Cr(Mo) in DS NiAl-(34-x)Cr-xMo changes from $\langle 100 \rangle$ to $\langle 111 \rangle$ when $x \geq 0.7$ pct, which would mean that both phases are oriented favorably for dislocation slip in the present Ni-33Al-33Cr-1Mo alloy. Furthermore, deformation studies of NiAl single crystals[2,21,22] have shown that even the hard oriented $\langle 100 \rangle$ crystals are weak at elevated temperatures. Similarly, Stephens and Klopp[23] found that 230- and 90-μm grain size polycrystalline Cr had little creep resistance between 1089 and 1422 K. For example, the flow stress necessary for deformation at 10^{-7} s^{-1} and 1300 K in either [100] NiAl single crystals[2,20,21] or polycrystalline Cr[23,24] is about 10 MPa. Therefore, neither of these two phases can be considered to be the strong component providing the elevated temperature strength levels observed in DS NiAl-Cr(Mo) alloys (Figure 10).

With both NiAl and Cr being weak in themselves, we believe that the elevated temperature strength of DS NiAl-Cr(Mo) eutectics must derive from the reduced dimensions (O (1 μm)) of the fibers/lamella. For example, Raj and Pharr[25] demonstrated that strength is inversely proportional to the subgrain size, and Sherby *et al.*[26] have shown that increased creep strength is possible by artificially limiting the size of subgrains. Both Cr[23] and NiAl[21,26] will form subgrains during creep, and subgrain strengthening has been demonstrated NiAl.[27,28] Thus, it is possible that the enhanced elevated temperature properties of DS NiAl-Cr(Mo) alloys are, at least, partially due to subgrain strengthening of NiAl and/or Cr(Mo).

For alloys containing more than 0.7 at. pct Mo, the size of the subgrains in both phases must be limited by the lamellar boundaries. On the other hand, when Cr(Mo) fibers are grown in an NiAl matrix (Mo $<$ 0.7 at. pct), the size of subgrains in Cr(Mo) is limited by the fiber walls, while the subgrain size in NiAl is governed by the average intrafiber distance. Simple geometric calculations for DS NiAl-(33-x)Cr-xMo with a constant volume fraction of Cr(Mo) $\approx$ 0.35[3,19] indicate that the potential controlling phase is dependent on the microstructure. In the case of uniform cross section Cr fibers evenly distributed in a NiAl matrix (Mo $<$ 0.7 at. pct), the interfiber spacing is less than the fiber diameter; thus, deformation should be dictated by NiAl. However, when uniform lamella are formed (Mo $\geq$ 0.7 at. pct), the thickness of Cr(Mo) is about half that of NiAl, and subgrains in Cr(Mo) lamella should control strength. Because the current $\sim$1300 K data (Figure 9(a)) do not indicate an advantage for either microstructure, it is not presently possible to determine which phase has the most influence on deformation in DS NiAl-Cr(Mo) alloys.

A recent analysis of a 1273 K creep test of DS NiAl-34Cr[29] and testing of Cr particle strengthened NiAl-27Cr between 923 and 1373 K[30] indicate that few, if any, dislocations were present in Cr after elevated temperature deformation. Thus, it was concluded that Cr in these alloys behaved elastically, which is counter to the work of Stephens and Klopp,[23] who found Cr to be quite weak and readily deformable between 1089 and 1689 K. Additionally, Kolluru and Pollock[29] state that the NiAl dislocation structure found in crept DS NiAl-34Cr was the same as that found in single-phase NiAl, while Jimenez *et al.*[30] contend that the Cr particles help stabilize an effective, smaller than equilibrium, subgrain size, which led to strengthening *via* the mechanism described by Sherby *et al.*[26] Clearly, detailed transmission electron microscope studies of DS NiAl-(Cr,Mo) eutectics are needed to understand strengthening in these materials.

E. *Fibrous vs Lamellar Microstructure*

Based on the results in Figure 9, it is not clear that there is any positive effect on elevated temperature strength from a change in microstructure or alloying in DS NiAl-(34-x)Cr-xMo eutectics grown under the present Bridgman techniques: The equivalence of NiAl-34Cr and Ni-33Al-33Cr-1Mo at $\sim$1300 K (Figure 10(a)) indicates that both the fibrous and the lamellar structures have similar elevated temperature strengths. Furthermore, no solid solution or precipitation-hardening effects have resulted from the replacement of Cr by Mo because DS Ni-33Al-31Cr-3Mo is weaker than the alloys with 1 pct Mo (Figure 10(b)), while DS Ni-33Al-28Cr-6Mo has about the same strength as 1 pct Mo (Figure (10c)).

Both lamellar DS Ni-33Al-33Cr-1Mo (Figure 4) and Ni-33Al-31Cr-3Mo[4] possess room-temperature toughness of $\sim$16 MPa$\sqrt{\text{m}}$ over a wide range of directional solidification rate. If toughness were the only criteria, then the higher Mo content alloy would be a better choice because its toughness can be maintained to a faster growth rate (508 mm/h) compared with 1 pct Mo (127 mm/h). However, the loss of elevated temperature strength at the higher Mo content (Figure 10(b)) negates this growth rate advantage. As fibrous DS NiAl-34Cr[2] has also demonstrated a good toughness ($\sim$20 MPa$\sqrt{\text{m}}$) and its 1300 K strength is equivalent to that of Ni-33Al-33Cr-1Mo (Figure 10(a)), the NiAl-34Cr composition might be the best choice for development. This contention must be somewhat tempered because mechanical properties of DS NiAl-34Cr have not been investigated as a function of growth rate under modified Bridgman techniques. Additionally, because it is suggested by Table III that EDFG could result in much better elevated temperature strengths in lamellar Ni-33Al-33Cr-1Mo than fibrous NiAl-34Cr, more work with these two alloys and this directional solidification technique should be undertaken.

IV. SUMMARY OF RESULTS

A study of DS Ni-33Al-33Cr-1Mo by a modified Bridgman technique has shown the following.

1. Grain/cellular microstructures of lamellar NiAl and Cr(Mo) were formed after growth from 7.6 to 508 mm/h.
2. Neither dendrites nor third phases were observed after growth at any rate.
3. The best 1200 to 1400 K strength resulted from alloys DS between 25.4 and 254 mm/h.
4. Room-temperature toughness was about 16 MPa$\sqrt{\text{m}}$ for alloys grown between 12.7 and 127 mm/h.

Therefore, the Ni-33Al-33Cr-1Mo eutectic system can be DS over an order of magnitude in growth rates (12.7 and 127 mm/h) while maintaining a stable room-temperature toughness and good elevated temperature strength. However, comparison of the elevated temperature and room-temperature toughness properties of lamellar DS Ni-33-33Al-1Mo to the values reported in the literature for fibrous DS NiAl-34Cr reveal that a lamellar microstructure does not have inherently better properties than a fibrous structure.

REFERENCES

1. J.L. Walter and H.E. Cline: *Metall. Trans.*, 1970, vol. 1, pp. 1221-29.
2. D.R. Johnson, X.F. Chen, B.F. Oliver, R.D. Noebe, and J.D. Whittenberger: *Intermetallics*, 1995, vol. 3, pp. 99-113.
3. J.M. Yang, S.M. Jeng, K. Bain, and R.A. Amato: *Acta Mater.*, 1997, vol. 45, pp. 295-305.
4. J.D. Whittenberger, S.V. Raj, I.E. Locci, and J.A. Salem: *Intermetallics*, 1999, vol. 7, pp. 1159-68.
5. J.D. Cotton, R.D. Noebe, and M.J. Kaufman: *Structural Intermetallics*, R. Darolia, J.J. Lewandowski, C.T. Liu, P.L. Martin, D.B. Miracle, and M.V. Nathal, eds., TMS, Warrendale, PA, 1993, pp. 513-22.
6. H.E. Cline and J.L. Walter: *Metall. Trans.*, 1970, vol. 1, pp. 2907-17.
7. S.M. Joslin: Ph.D. Thesis, The University of Tennessee, Knoxville, TN, 1995.
8. J.M. Yang: *JOM*, 1997, vol. 49 (8), pp. 40-43.
9. J.D. Whittenberger, R.D. Noebe, D.R. Johnson, and B.F. Oliver: *Intermetallics*, 1997, vol. 5, pp. 173-84.
10. S.V. Raj, I.E. Locci, and J.D. Whittenberger: *Creep Behavior of Advanced Materials for the 21st Century*, R.S. Mishra, A.K. Mukherjee, and K. Linga Murty, eds., TMS, Warrendale, PA, 1999, pp. 295-310.
11. J. Daniel Whittenberger, S.V. Raj, and Ivan E. Locci: MRS paper, MRS, Pittsburgh, PA, 2001
12. "Standard Test Method for Plane-Strain Fracture Toughness of Metallic Materials," Test Method E 399-90, *Annual Book of ASTM Standards*, 03.01, ASTM, West Conshohocken, PA, 1990.
13. J.A. Salem, L.J. Ghosn, and M.G. Jenkins: *Ceram. Eng. Sci. Proc.*, 1998, vol. 19, pp. 587-94.
14. "Standard Test Method for Fracture Toughness of Advanced Ceramics," Test Method PS070, *Annual Book of ASTM Standards*, 15.01 ASTM, West Conshohocken, PA, 1998.
15. S.V. Raj and I.E. Locci: *Intermetallics*, 2001, vol. 9, pp. 217-27.
16. H.E. Cline, J.L. Walter, E. Lifshin, and R.R. Russell: *Metall. Trans.*, 1971, vol. 2, pp. 189-94.
17. R.D. Noebe, R.R. Bowman, and M.V. Nathal: *Int. Mater. Rev.*, 1993, vol. 38, pp. 193-232.
18. A. Misra, Z.L. Zu, R. Gabala, R.D. Noebe, and B.F. Oliver: *Structural Intermetallics*, M.V. Nathal, R. Darolia, C.T. Liu, P.L. Martin, D.B. Miracle, R. Wagner, and M. Yamaguchi, eds., TMS, Warrendale, PA, 1997, pp. 673-82.
19. T.M. Pollock and D. Kolluru: *Micromechanics of Advanced Materials*, S.N.G. Chu, P.K. Law, R.J. Arsenault, K. Sadananda, K.S. Chan, W.W. Gerberich, C.C. Chau, and T.M. Kung, TMS, Warrendale, PA, 1995, pp. 205-12.
20. J. Daniel Whittenberger, S.V. Raj, and I.E. Locci: *Creep Deformation: Fundamentals and Applications*, R.S. Mishra, J.C. Earthman, and S.V. Raj, eds., TMS, Warrendale, PA, 2002 pp. 331-41.
21. K.R. Forbes, U. Glatzel, R. Darolia, and W.D. Nix: in *High Temperature Ordered Intermetallics—V*, I. Baker, R. Darolia, J.D. Whittenberger, and M.H. Yoo, eds., Materials Research Society, Pittsburgh, PA, 1993, vol. 288, pp. 45-57.
22. J.D. Whittenberger, I.E. Locci, Ram Darolia, and R. Bowman: *Mater. Sci. Eng., A*, 1999, vol. A268, pp. 165-83.
23. J.R. Stephens and W.D. Klopp: *J. Less-Common Met.*, 1972, vol. 27, pp. 87-94.
24. J. Daniel Whittenberger, Beverly Aikin, and Jon Salem: unpublished research.
25. S.V. Raj and G.M. Phaar: *Mater. Sci. Eng.*, 1986, vol. 81, pp. 217-37.
26. O.D. Sherby, R.H. Klundt, and A.K. Miller: *Metall. Trans. A*, 1977, vol. 8A, pp. 843-50.
27. J.D. Whittenberger: *J. Mater. Sci.*, 1987, vol. 22, pp. 394-402.
28. J.D. Whittenberger, R.D. Noebe, and A. Garg: *Metall. Mater. Trans. A*, 1996, vol. 27A, pp. 3170-80.
29. D.V. Kolluru and T.M. Pollock: *Acta Mater.*, 1998, vol. 46, pp. 2859-76.
30. J.A. Jimenez, S. Klaus, M. Carsi, O.A. Ruano, and G. Frommeyer: *Acta Mater.*, 1999, vol. 47, pp. 3655-62.